

## New Tetraazaannulene Hosts for Fullerenes

Jimmy U. Franco, Justin C. Hammons, Daniel Rios, and Marilyn M. Olmstead\*

Department of Chemistry, University of California, Davis, California 95616

Received February 7, 2010

Two modifications to the doubly concaved host molecules based on well-known nickel tetraazaannulene complexes have resulted in the preparation of the compounds Ni(NapTMTAA)·2benzene, 1,6,8,15,17-tetramethyldinaphthalene-5,9,14,18-tetraazacyclotetradecinatonicel(II), and Ni(Cl<sub>4</sub>TMTAA)·CH<sub>2</sub>Cl<sub>2</sub>, 2,3,11,12-tetrachloro-6,8,15,17-tetramethyldibenzo-5,9,14,18-tetraazacyclotetradecinatonicel(II). When crystallized with C<sub>60</sub> in carbon disulfide, the crystalline, well-ordered, host–guest compounds Ni(NapTMTAA)·C<sub>60</sub>·2CS<sub>2</sub> and Ni(Cl<sub>4</sub>TMTAA)·C<sub>60</sub>·2CS<sub>2</sub> were formed. The compounds were characterized by X-ray crystallography. The crystal structures of the precursor host molecules showed very strong host–host interactions, particularly in the case of Ni(Cl<sub>4</sub>TMTAA), which had short Ni···Ni interactions of 3.3860(11) and 3.5888(11) Å in the two different dimers in the asymmetric unit; yet, these host–host interactions were entirely destroyed in the resultant host–guest compounds, and C<sub>60</sub> molecules were shown to make use of both cusps of the host macrocycle in the formation of a shape-selective arrangement.

### Introduction

Cocrystallization is a vital tool for the successful determination of crystal structures in fullerene crystallography.<sup>1–5</sup> Not only can the agent, or host, be used in cocrystallization to assist in crystallization, it can sometimes, but not always, eliminate the severe rotational disorder that is otherwise common in neat fullerene structures. The host also increases the mass of material involved in crystal formation and allows for the production of more numerous crystals, especially valuable in those cases (e.g., higher fullerenes, endohedral fullerenes) where only a few milligrams of fullerene are available. A further advantage lies in the flexibility in the choice of the host itself, which can be tailored for specific purposes such as the introduction of a heavy atom to help phase the structure or in the design of photoactive centers. The technique of cocrystallization has been in use since the early days of fullerene chemistry either by design or simply by the accidental occurrence of solvent molecules in the structures, particularly

benzene,<sup>6</sup> toluene,<sup>7</sup> xylenes,<sup>8</sup> and more extensive aromatic molecules. The design of various types of molecules that form complexes with fullerenes is an active research area and the subject of numerous reviews.<sup>9–11</sup> Modifications to the host molecules for guest fullerenes in order to extend the  $\pi$ – $\pi$  interactions include the strategies of increasing the number of benzene rings,<sup>11</sup> addition of benzylic substituents to the nickel macrocycle NiTMTAA,<sup>12</sup> increasing the numbers of peripheral TTF (tetrathiafulvalene) groups,<sup>11</sup> and modification of the cavity formed by carbon nano-rings by substitution of phenyl by naphthalene units.<sup>10</sup> Clearly, aromaticity in the host molecule enhances van der Waals or dispersive intermolecular interactions between itself and the guest fullerene. Increasing the concavity match to the fullerene surface has been very successfully employed in many studies, although it should be noted that even interactions between fullerenes and the flat surfaces of porphyrin molecules have been shown to be quite strong.<sup>13–16</sup> In addition to  $\pi$ ··· $\pi$  interactions,  $n$ ··· $\pi$  interactions and electrostatic interactions comprise important intermolecular forces in the structures containing fullerene

\*To whom correspondence should be addressed. E-mail: mmolmstead@ucdavis.edu.

(1) Atwood, J. L.; Barbour, L. J.; Raston, C. L. *Cryst. Growth Des.* 2002, 2, 3.

(2) Atwood, J. L.; Barbour, L. J.; Heaven, M. W.; Raston, C. L. *Chem. Commun.* 2003, 2270.

(3) Sygula, A.; Fronczek, F. R.; Sygula, R.; Rabideau, P. W.; Olmstead, M. M. *J. Am. Chem. Soc.* 2008, 129, 3842.

(4) Georghiou, P. E.; Dawe, L. N.; Tran, H.-A.; Strübe, J.; Neumann, B.; Stammeler, H.-G.; Kuck, D. *J. Org. Chem.* 2008, 73, 9040.

(5) Balch, A. L.; Olmstead, M. M. *Coord. Chem. Rev.* 1999, 185, 601.

(6) Balch, A. L.; Lee, J. W.; Noll, B. C.; Olmstead, M. M. *Chem. Commun.* 1993, 56.

(7) Troshin, P. A.; Prisyazhnik, V. V.; Troyanov, S. I.; Boltalina, O. V.; Mackeyev, Y. A.; Kyrikova, M. A. *Proc. Electrochem. Soc.* 2001, 11, 548.

(8) Stevenson, S.; Lee, H. M.; Olmstead, M. M.; Kozikowski, C.; Stevenson, P.; Balch, A. L. *Chem.—Eur. J.* 2002, 8, 4528.

(9) Makha, M.; Purich, A.; Raston, C. L.; Sobolev, A. N. *Eur. J. Inorg. Chem.* 2006, 507.

(10) Pérez, E. M.; Martin, N. *Chem. Soc. Rev.* 2008, 37, 1512.

(11) Pérez, E. M.; Illescas, B. M.; Herranz, M. A.; Martin, N. *New J. Chem.* 2009, 33, 228.

(12) Norret, M.; Makha, M.; Sobolev, A. N.; Raston, C. L. *New J. Chem.* 2008, 32, 808.

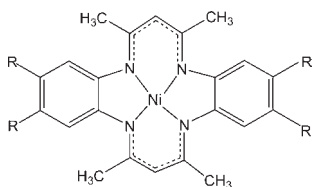
(13) Olmstead, M. M.; Costa, D. A.; Maitra, K.; Noll, B. C.; Phillips, S. L.; Van Calcar, P. M.; Balch, A. L. *J. Am. Chem. Soc.* 1999, 121, 7090.

(14) Wang, Y.-B.; Lin, Z. *J. Am. Chem. Soc.* 2003, 125, 6072.

(15) Beavers, C. M.; Chaur., M.; Olmstead, M. M.; Echegoyen, L.; Balch., A. L. *J. Am. Chem. Soc.* 2009, 131, 11519.

(16) Vilmercati, P.; Castellarin-Cudia, C.; Gebauer, R.; Ghosh, P.; Lizzit, S.; Petaccia, L.; Cepek, C.; Larciprete, R.; Verdini, A.; Floreano, L.; Morganta, A.; Goldoni, A. *J. Am. Chem. Soc.* 2009, 131, 664.

## Scheme 1



molecules. In this study we examine two modifications to the earlier reported tetraazaannulene cocrystallization agent shown in Scheme 1.

TMTAA ( $R = H$ ) and OMTAA ( $R = Me$ ) are doubly concave macrocycles whose use as hosts for globular molecules such as  $C_{60}$ , phosphorus sulfide, and carboranes was developed within the last 10 years.<sup>17–23</sup> One of our modifications extends the molecule's  $\pi$  system in the longer dimension by substitution with naphthalene. The other modification has  $R = Cl$ , which alters the molecule electrostatically. Our impetus for these studies was to produce new hosts for use in the crystallography of large fullerenes. We began this study by determination of the structures of the host molecules themselves,  $Ni(NapTMTAA) \cdot 2benzene$ , **1**, and  $Ni(Cl_4TMTAA) \cdot CH_2Cl_2$ , **3**, and subsequently determined the structures of their cocrystals with  $C_{60}$ , namely,  $Ni(NapTMTAA) \cdot C_{60} \cdot 2CS_2$ , **2**, and  $Ni(Cl_4TMTAA) \cdot C_{60} \cdot 2CS_2$ , **4**. As will be shown, all of these structures were well-ordered with interesting intermolecular interactions.

## Results

Synthesis of the host molecules is a templated Schiff base condensation that readily leads to the tetraazaannulenes in structures **1** and **3**, as depicted in Scheme 2. In the reaction with acetylacetone, use of diamionaphthalene instead of diaminobenzene extends the phenyl "arm" in the dimension shown. For the tetrachloro derivative, acetylacetone is reacted with 1,2-diamino-4,5-dichlorobenzene. Both modifications of the macrocycle are doubly concave, as seen in earlier studies, since the curvature is generated by steric interactions between ortho hydrogens on the phenyl or naphthyl ring and the methyl groups on the phenylene portion.

**Description of Structures.**  $Ni(NapTMTAA) \cdot 2benzene$ , **1**. Crystals of the naphthalene-based Schiff base form with two independent molecules of the Ni complex and four molecules of benzene in the asymmetric unit. One of the benzene molecules is disordered. Each of the Ni complexes exhibits similar double curvature in the macrocyclic ligand. The larger cusp contains the naphthalene rings. The structure of one of these complexes is depicted in Figure 1. The saddle shape allows for hydrogens on C15, C30, C22, and C23 to

avoid the methyl hydrogens on C31, C32, C33, and C34. The crystal packing is a striking example of complementarity of molecular shapes.

A predominant motif is illustrated in Figure 2. The two molecules do not exactly overlap but are offset such that the larger of the two cusps overlaps. The  $Ni1 \cdots Ni2$  distance is 4.5848(5) Å. From Figure 2 it is obvious how spherical molecules like  $C_{60}$  could occupy guest positions with  $Ni(NapTMTAA)$  as a host. Further, it is apparent that there are two distinct concavities, one narrow and one wide. In the host–guest ( $C_{60}$ ) crystal, **2**, both surfaces are used. The strong intermolecular interactions between  $Ni(NapTMTAA)$  molecules effectively exclude the benzene molecules from occupying any intercalated positions, and the benzenes do not participate in any  $\pi \cdots \pi$  stacking.

$Ni(NapTMTAA) \cdot C_{60} \cdot 2CS_2$ , **2**. Cocrystallization of  $Ni(NapTMTAA)$  with  $C_{60}$  in  $CS_2$  leads to a structure with  $C_{60}$  fitting into both large and small cusps of the host Ni complex. It is unusual for  $C_{60}$  to crystallize with high crystallographic symmetry and no disorder, but it does so in this structure. The crystal system is orthorhombic, space group  $Pmnm$ , with  $Z = 4$ . Both  $C_{60}$  and  $Ni(NapTMTAA)$  have crystallographic  $mm2$  symmetry; thus the asymmetric unit contains two one-quarter molecules of each. One of the  $CS_2$  molecules is disordered such that an S atom is shared between two different orientations. A portion of the packing is shown in Figure 3. A slightly closer contact between  $Ni(NapTMTAA)$  and a carbon atom of  $C_{60}$  occurs on the side with the smaller cusp, 3.236 vs 3.371 Å. Both shape selectivity and  $\pi \cdots \pi$  intermolecular interactions contribute to the optimal arrangement. The packing in the  $bc$  plane, as shown in Figure 4, places the  $C_{60}$ 's in a sawtooth, or zigzag, arrangement with center–center separations of 10.266 Å and a center–center–center angle of 112.4°. This is the most common arrangement for close contacts between  $C_{60}$  molecules in host–guest crystals.<sup>9</sup> In the next layer, in the  $a$  direction,  $CS_2$  molecules and  $C_{60}$ 's alternate in their positions.

$Ni(Cl_4TMTAA) \cdot CH_2Cl_2$ , **3**. Modification of the TMAA ligand with four Cl's yields another Ni complex,  $Ni(Cl_4TMTAA)$ , that has a  $-+++$ -polar character as well as a delocalized  $\pi$  system and a double saddle conformation. Evidently, this change in polarity enhances the intermolecular interactions between like molecules, as shown in Figures 5 and 6. A remarkable feature of the dimers is the short  $Ni \cdots Ni$  distance, 3.3860(11) Å for  $Ni1 \cdots Ni2$  and somewhat longer, 3.5888(11) Å, for  $Ni3 \cdots Ni4$ . The overlap of the two molecules in  $Ni(Cl_4TMTAA)$  is more intimate than in  $Ni(NapTMTAA)$ . The curvatures closely follow one on the other, but with the small cusp overlapping the large cusp and *vice versa*. Thus, instead of being congruent, one molecule is rotated by 90° with respect to the other. This brings the Ni's into close contact. Although metallophilic interactions are well-known for Ag and Au, such interactions between Ni's are less common but are known. The variation in  $Ni \cdots Ni$  separations highlights the fact that these are probably only weakly attractive interactions. In addition to  $\pi \cdots \pi$  overlap, this distinct arrangement achieves an alternation of Cl's in such a way as to minimize repulsions between them, as shown in Figure 6.

(17) Ishii, T.; Aizawa, N.; Kanehama, R.; Yamashita, M.; Matsuzaka, H.; Kodama, T.; Kikuchi, K.; Ikemoto, I. *Inorg. Chim. Acta* **2001**, *317*, 81.

(18) Andrews, P. C.; Atwood, J. L.; Barbour, L. J.; Nichols, P. J.; Raston, C. L. *Chem.—Eur. J.* **1998**, *1384*.

(19) Andrews, P. C.; Atwood, J. L.; Barbour, L. J.; Croucher, P. D.; Nichols, P. J.; Smith, N. O.; Skelton, B. W.; White, A. H.; Raston, C. L. *J. Chem. Soc., Dalton Trans.* **1999**, 2927.

(20) Boyd, P. D. W.; Hodgson, M. C.; Rickard, C. E. F.; Oliver, A. G.; Chaker, L.; Brothers, P. J.; Boiskar, R. D.; Tham, F. S.; Reed, C. A. *J. Am. Chem. Soc.* **1999**, *121*, 10487.

(21) Croucher, P. D.; Marshall, J. M. E.; Nichols, P. J.; Raston, C. L. *Chem. Commun.* **1999**, 193.

(22) Soldatov, D. V.; Diamante, P. R.; Ratcliffe, C. I.; Ripmeester, J. A. *Inorg. Chem.* **2001**, *40*, 5660.

(23) Ishii, T.; Aizawa, N.; Kanehama, R.; Yamashita, M.; Sugiura, K.; Miyaska, H. *Coord. Chem. Rev.* **2002**, *226*, 113.

Scheme 2

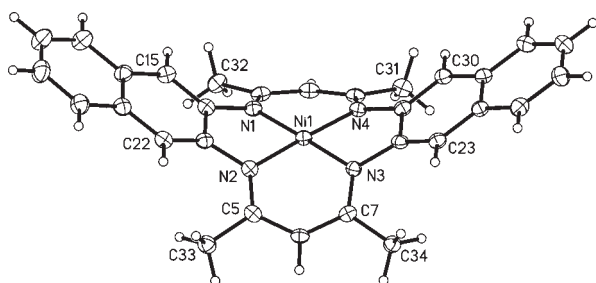
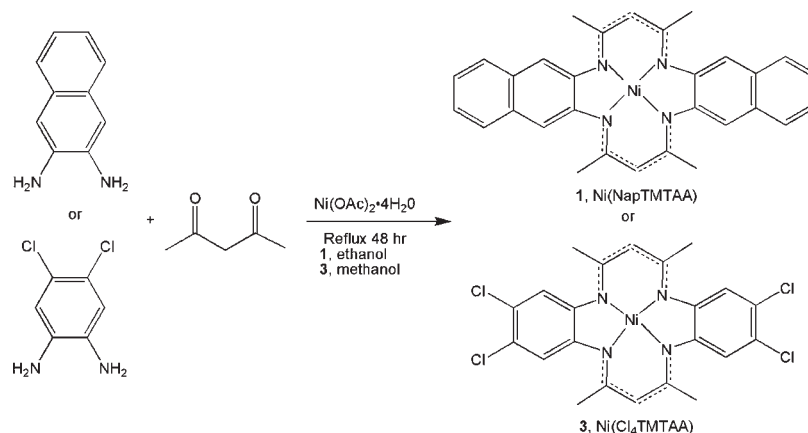


**Figure 1.** View of  $\text{Ni}(\text{NapTMTAA})$  with thermal ellipsoids drawn at the 50% probability level.

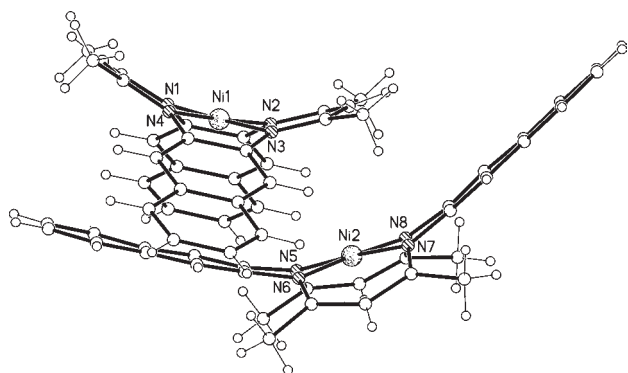


**Figure 2.** Overlapping arrangement of adjacent molecules of  $\text{Ni}(\text{NapTMTAA})$ .

$\text{Ni}(\text{Cl}_4\text{TMTAA}) \cdot \text{C}_{60} \cdot 2\text{CS}_2$ , **4**. Well-formed crystals that contain three molecular components arise when equimolar  $\text{CS}_2$  solutions of  $\text{Ni}(\text{Cl}_4\text{TMTAA})$  and  $\text{C}_{60}$  are allowed to mix in a 5 mm tube. The crystal structure has one half molecule of  $\text{Ni}(\text{Cl}_4\text{TMTAA})$ , one half molecule of  $\text{C}_{60}$ , and a molecule of  $\text{CS}_2$  in the asymmetric unit. The full molecules are generated by a common crystallographic 2-fold axis, as shown in Figure 7. The structure of  $\text{C}_{60}$  in **4** represents another example of a structure of an underivatized fullerene that is fully ordered in its structure. The average standard uncertainty (su) in a C–C bond of the  $\text{C}_{60}$  is 0.003 Å. The C–C distances fall into two groups, namely, 6:6 and 6:5 ring junctions, and the bond distances average 1.388[4] and 1.453[6] Å, respectively (average deviations from the mean are given in square brackets). Not just one but both the large and

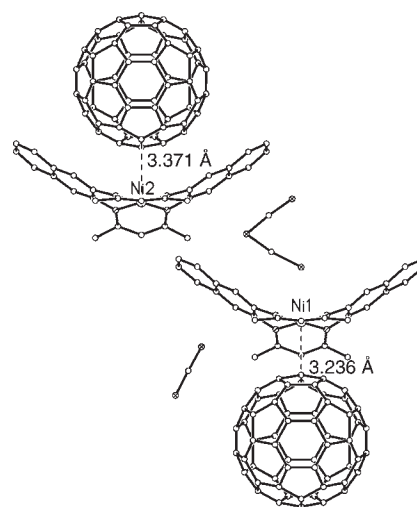


**Figure 3.** The affinity of  $\text{Ni}(\text{NapTMTAA})$  for  $\text{C}_{60}$  is enhanced by interaction with both the major and minor cusps of the host molecule. Disorder in one of the two  $\text{CS}_2$  solvate molecules is also shown.

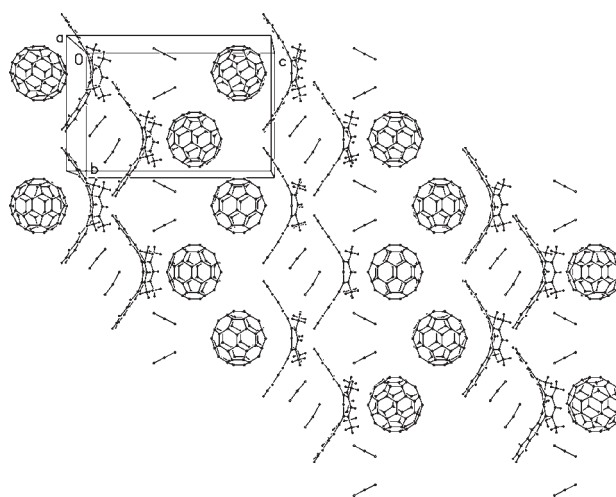


**Figure 4.** Packing of the structure of  $\text{Ni}(\text{NapTMTAA}) \cdot \text{C}_{60} \cdot 2\text{CS}_2$ , **2** in the  $bc$  plane.

small cusps of the ligand encapsulate the  $\text{C}_{60}$ . This is clearly seen in a view down the  $c$  axis shown in Figure 8. The closest contacts to Ni are to midpoints of 6:6 junctions,

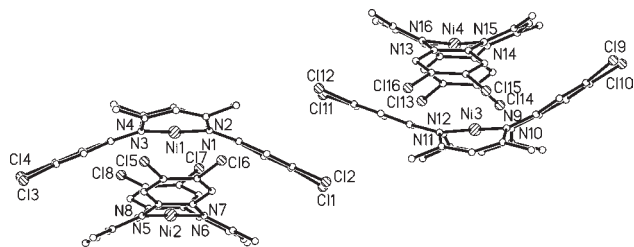


**Figure 5.** View of the stacking of Ni complexes and dimer formation.

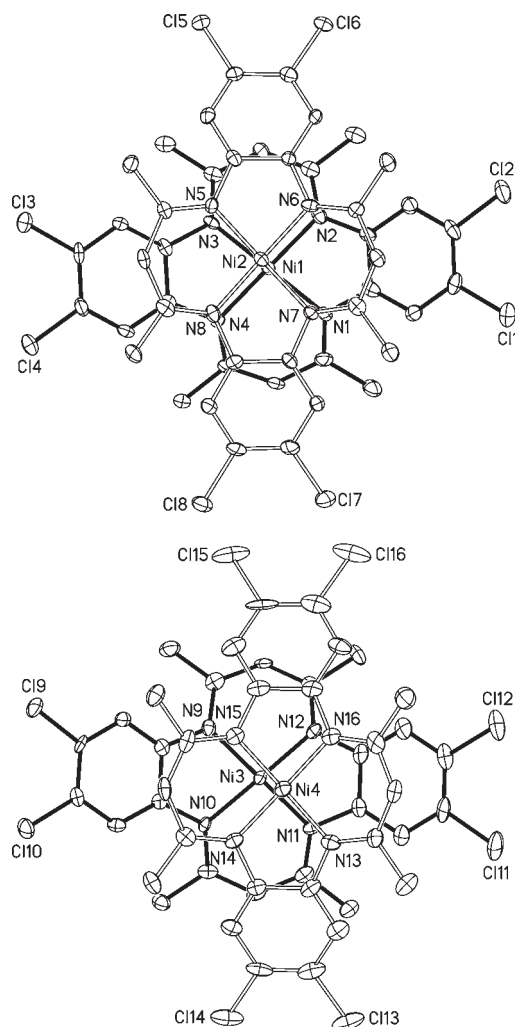


**Figure 6.** View of the stacking interaction of the two different dimers in the structure of  $\text{Ni}(\text{Cl}_4\text{TMTAA})$ . The view is perpendicular to the least-squares plane of N1/N2/N3/N4 (top) and N9/N10/N11/N12 (bottom). Thermal ellipsoids are drawn at the 50% probability level.

the regions of higher  $\pi$  electron density. The intermolecular contacts are similar; on the large cusp side, the distance  $\text{Ni} \cdots \text{C43/C43A}$  midpoint is 3.130(4) Å, and on the small cusp side the  $\text{Ni} \cdots \text{C34B/C34C}$  midpoint it is 3.126(4) Å. From the viewpoint of electrostatic interactions, some short  $\text{Cl} \cdots \text{C}(\text{C}_{60})$  contacts also occur in the range 3.409 to 3.510 Å. These are reminiscent of those seen in the well-ordered cocrystal of  $\text{C}_{60}$  and perchloroazatriquinacene (range 3.28–3.48 Å).<sup>24</sup> Thus, both

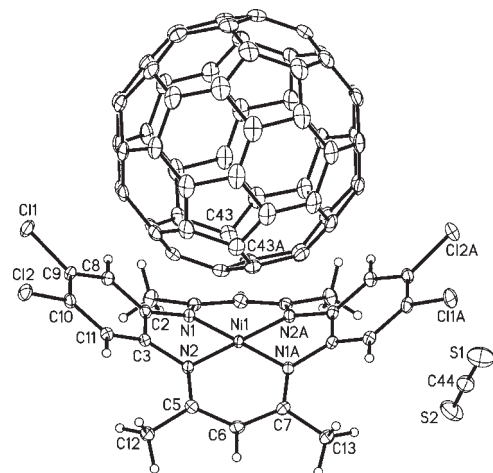


**Figure 7.** View of the structure of  $\text{Ni}(\text{Cl}_4\text{TMTAA}) \cdot \text{C}_{60} \cdot 2\text{CS}_2$ , **4**. Thermal ellipsoids are drawn at the 50% probability level. The crystallographic 2-fold axis bisects the C43/C43A bond and passes through Ni1.

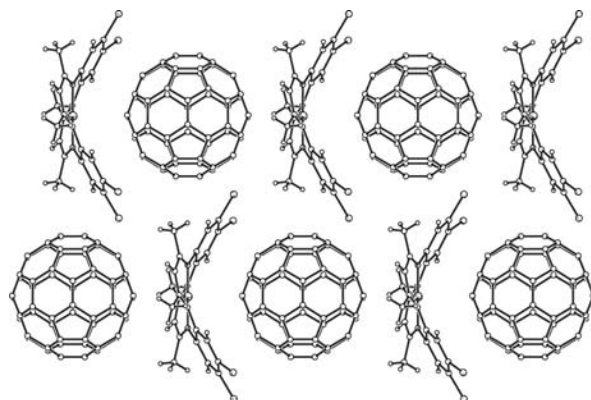


**Figure 8.** View of the alternating layers of  $\text{Ni}(\text{Cl}_4\text{TMTAA})$  and  $\text{C}_{60}$  in **4**.

$\pi \cdots \pi$  and  $n \cdots \pi$  interactions appear to contribute to the fixed orientation of  $\text{C}_{60}$  in this structure. The  $\text{CS}_2$  molecules occupy interstitial positions.

The structure of **4** (collected at 90 K) is isostructural to a structure<sup>25</sup> of  $\text{Ni}(\text{OMTAA}) \cdot \text{C}_{60} \cdot 2\text{CS}_2$  (collected at 123 K) in which all four Cl atoms are replaced by  $\text{CH}_3$  groups. Here, the authors have described the  $\text{Ni} \cdots \text{C}_{60}$  interaction to be stronger on the phenyl side (large cusp), but, according to the published coordinates, the contact distances to the midpoints of the C–C bonds on the 2-fold axis are 3.17(1) Å for the large cusp and 3.16(1) Å for the small cusp. Thus, in both structures, there is a slight preference for association with  $\text{C}_{60}$  at the smaller cusp. The greater electron-withdrawing effect of the chlorides than the methyl groups may strengthen the acceptor ability of the Ni complex. In both structures,  $\text{C}_{60} \cdots \text{C}_{60}$  contacts are near the van der Waals limit: the shortest center-to-center distances are 10.004 Å for  $\text{Ni}(\text{Cl}_4\text{TMTAA}) \cdot \text{C}_{60} \cdot 2\text{CS}_2$  and 10.038 Å for  $\text{Ni}(\text{OMTAA}) \cdot \text{C}_{60} \cdot 2\text{CS}_2$ . The arrangement of  $\text{C}_{60}$ 's in close proximity is also a zigzag, as seen for **2**; however it is closer to linear. The center–center angle in **4** is 155.8°.

(24) Pham, D.; Bertran, J. C.; Olmstead, M. M.; Mascal, M.; Balch, A. L. *Org. Lett.* **2005**, *7*, 2805.

(25) Croucher, P. D.; Nichols, P. J.; Raston, C. L. *J. Chem. Soc., Dalton Trans.* **1999**, 279.



Table 1. Crystal Data

	Ni(NapTMTAA)·2benzene	Ni(NapTMTAA)·C <sub>60</sub> ·2CS <sub>2</sub>	Ni(Cl <sub>4</sub> TMTAA)·CH <sub>2</sub> Cl <sub>2</sub>	Ni(Cl <sub>4</sub> TMTAA)·C <sub>60</sub> ·2CS <sub>2</sub>
compound	<b>1</b>	<b>2</b>	<b>3</b>	<b>4</b>
formula	C <sub>42</sub> H <sub>38</sub> N <sub>4</sub> Ni	C <sub>92</sub> H <sub>26</sub> N <sub>4</sub> NiS <sub>4</sub>	C <sub>23</sub> H <sub>20</sub> Cl <sub>6</sub> N <sub>4</sub> Ni	C <sub>84</sub> H <sub>18</sub> Cl <sub>4</sub> N <sub>4</sub> NiS <sub>4</sub>
fw	657.47	1374.12	623.82	1411.77
color, habit	dark green block	black plate	green-black parallelepiped	black plate
cryst syst	monoclinic	orthorhombic	triclinic	monoclinic
space group	C2/c	Pmmm	P $\bar{1}$	C2/c
a, Å	26.1470(16)	12.6509(11)	14.017(3)	21.6523(15)
b, Å	21.2466(16)	17.0655(14)	16.479(3)	13.1967(9)
c, Å	23.8863(15)	25.783(2)	22.848(4)	19.5618(13)
α, deg			73.985(3)	
β, deg	95.371(3)		80.445(3)	106.583(3)
γ, deg			76.468(3)	
V, Å <sup>3</sup>	13211.4(15)	5566.4(8)	4902.8(16)	5357.1(6)
Z	16	4	8	4
unique data	16 677 [R(int) = 0.073]	6887 [R(int) = 0.058]	18 677 [R(int) = 0.117]	6136 [R(int) = 0.024]
obsd data (I > 2σ(I))	10 830	5153	12 695	5456
R1 (obsd data)	0.0475	0.0641	0.0540	0.0347
wR2 (all data)	0.1416	0.1730	0.1173	0.0961

The precursor molecules of Ni(Cl<sub>4</sub>TMTAA) and Ni(OMTAA) have different structures. Both Ni(OMTAA)<sup>25</sup> and the free ligand, OMTAAH<sub>2</sub>,<sup>26</sup> crystallize without solvent and are isostructural. Their structures are characterized by strong  $\pi$  stacking that is more offset from the molecular center than seen in Ni(Cl<sub>4</sub>TMTAA)·CH<sub>2</sub>Cl<sub>2</sub>, **3**. There are no close Ni···Ni contacts in the structure of Ni(OMTAA); the shortest is 5.182 Å. Although **3** is a solvate and, of course, polymorphs may occur, the observation of close Ni···Ni contacts in **3** points to a subtle electronic difference from the methyl derivative.

## Discussion

If the aim of cocrystallization is the production of crystals that are better ordered in the solid state than their constituents, this aim can be stymied by disorder with respect to the site symmetry that is dictated by the host. This has been a recurrent problem for fullerene structures, which are always rotationally disordered in the absence of a host, but can have residual disorder even in the presence of host, especially if the host molecule has a symmetry of its own. Thus, a great deal of effort has been expended in the quest for a host molecule that will yield reliable, nondisordered fullerene structures; however, while elegant hosts have been designed, no one molecule has proven to be successful. We have presented two structures where cooperation among the attributes of molecular size, shape, and intermolecular interactions has allowed the site symmetry of the host to match some of the symmetry elements of C<sub>60</sub>. Tetraannulene molecules exhibit strong host–host interactions in the solid state.<sup>27</sup> In order for C<sub>60</sub> to cocrystallize with a tetraannulene molecule, it must afford host–guest interactions comparable in energy to those being lost in the host–host crystal. The electron-rich nature of the delocalized  $\pi$  system in both hosts presented here, Ni(NapTMTAA) and Ni(Cl<sub>4</sub>TMTAA), provides the necessary donor ability for this to occur, even though the distribution of charge density differs in detail due to the chloro substitution (see Supporting Information). The crystal structures of compounds **2** and **4** and the lack of disorder attest to the

strength of these interactions. However, recently,<sup>28</sup> covalent rather than noncovalent interactions were revealed in a related structure of TMTAA with C<sub>60</sub>, namely, [ $\eta^2$ -C<sub>60</sub>]Fe-(TMTAA)], in which the Fe···C–C(centroid) distance was only 2.17 Å. Although stereochemically similar, this is a true adduct rather than a host–guest cocrystal.

## Experimental Section

**Materials.** Nickelous acetate, acetylacetone, 2,3-diaminonaphthalene, 1,2-diamino-4,5-dichlorobenzene, C<sub>60</sub>, and solvents were obtained from standard sources without further purification.

**Preparation of Ni(NapTMTAA)·2benzene, 1.** 6,8,15,17-Tetra-methylidynaphthalene-5,9,14,18-tetraazacyclotetradecinatonicel(II). 2,3-Diaminonaphthalene (1.0 g, 0.0063 mol) was placed in a 250 mL round-bottom flask with Ni(CH<sub>3</sub>CO<sub>2</sub>)<sub>2</sub>·4H<sub>2</sub>O (0.79 g, 0.0031 mol) and dissolved in 50 mL of ethanol. The mixture was heated to 50 °C for 10 min. Subsequently, acetylacetone (0.65 mL, 0.0063 mol) was slowly added to the solution. The reaction mixture was refluxed for 48 h. After cooling to room temperature, all volatiles were removed under vacuum. The resulting green solid was chromatographed on silica gel using dichloromethane as the eluent, to yield 64% of product material. Crystals suitable for X-ray diffraction were obtained by slow evaporation of a benzene solution in a 5 mm tube. The Supporting Information contains the <sup>1</sup>H and <sup>13</sup>NMR spectra of **1**.

**Preparation of Ni(NapTMTAA)·C<sub>60</sub>·2CS<sub>2</sub>, 2.** Cocrystals were grown from carbon disulfide solutions of NapTMTAA and C<sub>60</sub> in a 1:1 molar ratio in a 5 mm tube.

**Preparation of Ni(Cl<sub>4</sub>TMTAA)·CH<sub>2</sub>Cl<sub>2</sub>, 3.** 2,3,11,12-Tetra-chloro-6,8,15,17-tetramethyldibenzo-5,9,14,18-tetraazacyclotetradecinatonicel(II). 1,2-Diamino-4,5-dichlorobenzene (1.08 g, 0.01 mol) was placed in a 250 mL round-bottom flask with Ni(CH<sub>3</sub>CO<sub>2</sub>)<sub>2</sub>·4H<sub>2</sub>O (1.245 g, 0.005 mol) and dissolved in 50 mL of methanol. The solution was heated to 50 °C for 10 min. Subsequently, acetylacetone (1.0 g, 0.01 mol) was slowly added to the reaction mixture. The reaction mixture was refluxed for 48 h. Upon completion, the reaction was cooled to room temperature and all volatiles were removed under vacuum. The resulting green solid was chromatographed on silica gel using CH<sub>2</sub>Cl<sub>2</sub>/hexane (5:1) as the eluent. X-ray quality crystals were grown by slow diffusion of methanol into dichloromethane, yield 55%. The Supporting Information contains the <sup>1</sup>H NMR and MALDI spectra of **3**.

(26) Buzatu, D. A.; Nolan, S. P.; Stevens, E. D. *Acta Crystallogr. Sect. C* **1995**, *51*, 1855.

(27) Grolik, J.; Dominiak, P. M.; Sieroń, L.; Woźniak, K.; Eilmes, J. *Tetrahedron* **2008**, *7796*.

(28) Malic, N.; Nichols, P. J.; Makha, M.; Raston, C. L. *Cryst. Growth Des.* **2009**, *9*, 863.

**Preparation of  $\text{Ni}(\text{Cl}_4\text{TMTAA})\cdot\text{C}_{60}\cdot 2\text{CS}_2$ , **4**.** Cocrystals were grown from carbon disulfide solutions of  $\text{Cl}_4\text{TMTAA}$  and  $\text{C}_{60}$  in an approximate 1:1 molar ratio in a 5 mm tube.

**X-ray Crystallography and Data Collection.** The crystals were removed from the glass tubes in which they were grown together with a small amount of mother liquor and immediately coated with a hydrocarbon oil on a microscope slide. A suitable crystal of each compound was mounted on a glass fiber with silicone grease and placed in the cold stream of a Bruker SMART Apex II diffractometer. Data reduction was carried out with SAINT and corrected for absorption using SADABS.<sup>29</sup> The structure of  $\text{Ni}(\text{Cl}_4\text{TMTAA})\cdot\text{CH}_2\text{Cl}_2$ , **3**, was a pseudomerohedral twin with two components, twin parameter 0.4220(8), and the absorption correction was carried with the use of TWINABS.<sup>17</sup> The structures were solved with the use of SHELXS97 and refined with

(29) Bruker AXS. *APEX2, SAINT, SADABS, TWINABS*; Bruker AXS Inc.: Madison, WI, 2007.

(30) Sheldrick, G. M. *Acta Crystallogr., Sect. A* **2008**, *64*, 112.

SHELXL97.<sup>30</sup> Hydrogen atoms were added geometrically and refined with a riding model.

Crystal data and selected data collection and refinement parameters are presented in Table 1.

**Acknowledgment.** We thank the National Science Foundation (Grant CHE-0716843) for financial support and F. L. Boyles for assistance with the electron density potential surface calculations.

**Supporting Information Available:**  $^1\text{H}$  and  $^{13}\text{C}$  NMR spectra of the purified samples of  $\text{Ni}(\text{NapTMTAA})\cdot 2\text{benzene}$ , **1**;  $^1\text{H}$  NMR spectra and MS (MALDI) of  $\text{Ni}(\text{Cl}_4\text{TMTAA})\cdot\text{CH}_2\text{Cl}_2$ , **3**. X-ray crystallographic files in CIF format for  $\text{Ni}(\text{NapTMTAA})\cdot 2\text{benzene}$ , **1**,  $\text{Ni}(\text{NapTMTAA})\cdot\text{C}_{60}\cdot 2\text{CS}_2$ , **2**,  $\text{Ni}(\text{Cl}_4\text{TMTAA})\cdot\text{CH}_2\text{Cl}_2$ , **3**, and  $\text{Ni}(\text{Cl}_4\text{TMTAA})\cdot\text{C}_{60}\cdot 2\text{CS}_2$ , **4**. Gaussian03 RHF/3.21g electron density potential surfaces for  $\text{Ni}(\text{NapTMTAA})$  and  $\text{Ni}(\text{Cl}_4\text{TMTAA})$ . This material is available free of charge via the Internet at <http://pubs.acs.org>.